Nonlinear Magnetization Dynamics under Circularly Polarized Field

Giorgio Bertotti,[1] Claudio Serpico,[2] and Isaak D. Mayergoyz[3]
[1]*Istituto Elettrotecnico Nazionale Galileo Ferraris, Corso M. d'Azeglio 42, I-10125 Torino, Italy*
[2]*Department of Electrical Engineering, Università di Napoli "Federico II," I-80125 Napoli, Italy*
[3]*Department of Electrical and Computer Engineering, University of Maryland, College Park, Maryland 20742*
(Received 17 May 2000)

Exact analytical results are presented for the nonlinear large motion of the magnetization vector in a body with uniaxial symmetry subject to a circularly polarized field. The absence of chaos, the existence of pure time-harmonic magnetization modes with no generation of higher-order harmonics, and the existence of quasiperiodic magnetization modes with spontaneous breaking of the rotational symmetry are proven. Application to ferromagnetic resonance and connection with the Stoner-Wohlfarth model are discussed.

DOI: 10.1103/PhysRevLett.86.724 PACS numbers: 75.40.Gb, 76.50.+g

A free magnetic moment $\mathbf{m}$ precesses in the magnetic field $\mathbf{H}$ at the rate $d\mathbf{m}/dt = -\gamma\mathbf{m} \times \mathbf{H}$ ($\gamma > 0$ for electronic moments). A similar equation is at the root of the dynamics of the local magnetization $\mathbf{M}(\mathbf{r}, t)$ of a magnetized medium: $\partial\mathbf{M}/\partial t = -\gamma\mathbf{M} \times \mathbf{H}_{\rm eff}$. In this case, the effective field $\mathbf{H}_{\rm eff}$ is the (variational) derivative of the system free energy with respect to the magnetization. The motion conserves $|\mathbf{M}|$ and is nondissipative ($\mathbf{H}_{\rm eff} \cdot \partial\mathbf{M}/\partial t = 0$). Energy dissipation can be taken into account by additional phenomenological terms, chosen through heuristic considerations. In ferromagnets, exchange heavily penalizes states where $|\mathbf{M}|$ deviates from the thermodynamic saturation magnetization M_s. Thus, descriptions where $|\mathbf{M}|$ is conserved are of particular interest. In the Landau-Lifshitz equation, $\partial\mathbf{M}/\partial t = -\gamma\mathbf{M} \times \mathbf{H}_{\rm eff} - \gamma(\alpha/M_s)\mathbf{M} \times (\mathbf{M} \times \mathbf{H}_{\rm eff})$, whereas $\partial\mathbf{M}/\partial t = -\gamma\mathbf{M} \times \mathbf{H}_{\rm eff} + (\alpha/M_s)\mathbf{M} \times \partial\mathbf{M}/\partial t$ in the form proposed by Gilbert [1]. The two equations are mathematically equivalent. Gilbert's approach amounts to adding a Rayleigh dissipation function proportional to $\alpha(\partial\mathbf{M}/\partial t)^2$ to the Lagrangian of the system [2]. In the rest of this Letter, reference will be made to the dimensionless Landau-Lifshitz-Gilbert (LLG) equation

$$\frac{\partial\mathbf{m}}{\partial t} - \alpha\mathbf{m} \times \frac{\partial\mathbf{m}}{\partial t} = -\mathbf{m} \times \mathbf{h}_{\rm eff}\,, \qquad (1)$$

where time is measured in units of $(\gamma M_s)^{-1}$, $\mathbf{h}_{\rm eff} = \mathbf{H}_{\rm eff}/M_s$, $\mathbf{m} = \mathbf{M}/M_s$, and $\mathbf{m}$ has zero normal derivative at the body surface. It will be assumed that $\mathbf{h}_{\rm eff} = \mathbf{h}_a + \mathbf{h}_M + \mathbf{h}_{\rm AN} + \mathbf{h}_{\rm EX}$, where the applied field $\mathbf{h}_a$ is a given spatially uniform function of time, whereas the other terms represent the magnetostatic, anisotropy, and exchange fields, respectively.

The LLG equation is employed in most studies of the dynamics of ferromagnetic media. In particular, it plays a crucial role in the description of ferromagnetic resonance [3] and of magnetization switching in thin films [4]. The limits under which the phenomenological introduction of damping is acceptable and is in agreement with microscopic models of spin dynamics are still under study [1,5]. On the other hand, there exist few exact results about the properties of truly nonlinear large motions of $\mathbf{M}$. It is usually felt that the onset of coupled nonuniform modes should play an important role in the complex magnetization behavior observed in experiments [6,7], and that the appearance of chaos should be expected under broad conditions [3,8].

In this Letter it is shown that significant progress in the investigation of these issues can be achieved by considering the case where the system described by Eq. (1) exhibits rotational symmetry around a certain axis and the external field is circularly polarized in the perpendicular plane. Some aspects of this problem were considered in [9], without recognizing, however, the far-reaching implications of the symmetry assumption. In fact, it will be shown that, as a consequence of rotational invariance, there always exist *exact* uniform-mode solutions of Eq. (1) coupled to magnetostatic Maxwell equations. These modes are expected to be the main modes excited by uniform rotating fields whenever surface anisotropy is negligible and the excitation conditions preclude the existence of magnetic domains, nonuniform resonance modes [10], and Suhl's instabilities [6]. Interestingly, these uniform modes represent pure *time-harmonic magnetization modes* with no generation of higher-order harmonics despite the strongly nonlinear character of the problem. In addition, it will be shown that *quasiperiodic magnetization modes*, with spontaneous breaking of the rotational symmetry, necessarily set in when none of the time-harmonic modes is stable. From a slightly different perspective, the study of these modes represents the natural dynamic generalization of the classical Stoner-Wohlfarth model [11]. Several distinctive features, as, for example, the concept of astroid, are preserved by uniform-mode dynamics under rotating field. Finally, it is interesting to note that the rotational symmetry analysis may lead to substantial simplifications even in problems where exchange plays a role, as in conducting thin films [12].

Rotational symmetry results in the following conditions on the dynamics: (i) the dissipation parameter α of Eq. (1)

 0031-9007/01/86(4)/724(4)$15.00

is a positively defined function of $\mathbf{h}_{\mathrm{eff}}$ and $\mathbf{m}$ invariant with respect to rotations of the reference frame about the z axis; (ii) the body is of spheroidal shape, with symmetry axis along z; (iii) crystal anisotropy is uniaxial, i.e., $\mathbf{h}_{\mathrm{AN}} = (2K_1/\mu_0 M_s^2)\mathbf{e}_z$ ($\mathbf{e}_z$ is the unit vector along z); (iv) the external field is of the form $\mathbf{h}_a(t) = \mathbf{h}_{a\perp}(t) + h_{az}\mathbf{e}_z$ ($\perp$ indicates components in the plane perpendicular to $\mathbf{e}_z$), where h_{az} is constant, whereas $\mathbf{h}_{a\perp}(t)$ has constant amplitude $h_{a\perp}$ and is rotated with angular frequency ω. For uniform modes, $\mathbf{h}_{\mathrm{EX}} = 0$ and $\mathbf{h}_M = -N_\perp \mathbf{m}_\perp - N_z m_z \mathbf{e}_z$, where N_z and $N_\perp$ represent the z and $\perp$ demagnetizing factors, respectively. Therefore, apart from terms proportional to $\mathbf{m}$ that do not contribute to Eq. (1), $\mathbf{h}_{\mathrm{eff}} = \mathbf{h}_{a\perp}(t) + (h_{az} + \kappa_{\mathrm{eff}} m_z)\mathbf{e}_z$, where $\kappa_{\mathrm{eff}} = 2K_1/\mu_0 M_s^2 + N_\perp - N_z$. As a consequence of rotational symmetry, the description becomes remarkably simpler by passing to the *rotating frame of reference* in which the external field is stationary, and by using spherical coordinates (θ, ϕ) for $\mathbf{m}$. In other words, one looks for $\mathbf{m}$ in the form: $m_x = \sin\theta\cos(\omega t - \phi)$, $m_y = \sin\theta\sin(\omega t - \phi)$, $m_z = \cos\theta$, where θ and ϕ are functions of time and ϕ measures the lag of $\mathbf{m}_\perp$ with respect to $\mathbf{h}_{a\perp}$. In terms of (θ, ϕ), Eq. (1) becomes

$$\frac{d\theta}{dt} - \alpha \sin\theta \frac{d\phi}{dt} = \kappa_{\mathrm{eff}}[b_\perp \sin\phi - \Omega \sin\theta], \tag{2}$$

$$\alpha \frac{d\theta}{dt} + \sin\theta \frac{d\phi}{dt} = \kappa_{\mathrm{eff}}[b_\perp \cos\theta \cos\phi - (b_z + \cos\theta)\sin\theta], \tag{3}$$

where $b_z = (h_{az} - \omega)/\kappa_{\mathrm{eff}}$, $b_\perp = h_{a\perp}/\kappa_{\mathrm{eff}}$, $\Omega = \alpha\omega/\kappa_{\mathrm{eff}}$, and α is now a function of (θ, ϕ) with no explicit dependence on time.

Equations (2) and (3) describe an *autonomous dynamical system on the unit sphere*. This fact has some remarkable consequences on uniform-mode dynamics.

(i) *There must exist equilibrium states for the system,* because the $d\mathbf{m}/dt$ vector field on the sphere necessarily has singular points [13]. An equilibrium state in the rotating frame represents a magnetization mode rigidly rotating with the field. Therefore, the problem admits *exact time-harmonic solutions*, with no generation of higher-order harmonics, in spite of the inherent nonlinear character of the dynamics. These solutions will be termed $\mathbf{P}$-modes.

(ii) The number of $\mathbf{P}$-modes is *at least two and is even under all circumstances*. This conclusion derives from the Poincaré index theorem [13], which asserts that the number of nodes and foci minus the number of saddles of any autonomous dynamics on the sphere is equal to two.

(iii) *The onset of chaos is precluded*, because the phase space is two dimensional [14].

Exact analytical results are obtained when α and consequently Ω are just constants. $\mathbf{P}$-modes are calculated by equating the right-hand side (rhs) of Eqs. (2) and (3) to zero. By eliminating ϕ, one finds that $m_z = \cos\theta$ obeys the fourth-order polynomial equation

$$\frac{b_\perp^2}{1 - m_z^2} - \frac{(b_z + m_z)^2}{m_z^2} - \Omega^2 = 0. \tag{4}$$

All real m_z zeros of Eq. (4) are located in the interval $-1 \leq m_z \leq 1$. In general, one may expect zero, two, or four of them. However, the case of no zeros is forbidden by the index theorem [13]. Therefore, *only two situations are possible*, one with two and one with four $\mathbf{P}$-modes. Interestingly, although Eqs. (2) and (3) depend on five parameters, i.e., $(b_z, b_\perp, \Omega, \alpha, \kappa_{\mathrm{eff}})$, only $(b_z, |b_\perp|, |\Omega|)$ appear in Eq. (4). Hence, bodies characterized by different values of $(\alpha, \kappa_{\mathrm{eff}})$ *will exhibit identical* $\mathbf{P}$*-modes* whenever the set $(b_z, |b_\perp|, |\Omega|)$ takes identical values.

Equation (4) describes a hyperbolic line in the $(b_z, |b_\perp|)$ plane, a line that can be represented as

$$b_z = m_z(v - 1), \tag{5}$$

$$|b_\perp| = \sqrt{(1 - m_z^2)(v^2 + \Omega^2)}, \tag{6}$$

with $-\infty < v < +\infty$. Comparison with the rhs of Eqs. (2) and (3) shows that $v = \Omega\cot\phi$. Equations (5) and (6) define the field conditions that will produce a $\mathbf{P}$-mode with any desired (θ, ϕ) values.

$\mathbf{P}$-mode stability can be studied by considering small deviations from equilibrium $[\Delta\theta\exp(\lambda t), \Delta\phi\exp(\lambda t)]$ and by applying first-order perturbation theory to Eqs. (2) and (3), in order to reduce them to the standard eigenvalue form $Ax = \lambda x$, with $x = (\Delta\theta, \Delta\phi)$. Stability is controlled by the trace and the determinant of the matrix A. After some algebra, one finds

$$\det A = \frac{\kappa_{\mathrm{eff}}^2}{1 + \alpha^2}[v^2 - (1 - m_z^2)v + \Omega^2 m_z^2], \tag{7}$$

$$\mathrm{tr}A = -\frac{2\alpha\kappa_{\mathrm{eff}}}{1 + \alpha^2}\left[v - \frac{1 - m_z^2}{2} + \frac{\Omega m_z}{\alpha}\right], \tag{8}$$

where both $m_z = \cos\theta$ and $\Omega\cot\phi$ refer to the particular $\mathbf{P}$-mode considered. Three situations are of main interest [15]: stable nodes or foci ($\mathrm{tr}A < 0, \det A > 0$); unstable nodes or foci ($\mathrm{tr}A > 0, \det A > 0$); saddles ($\det A < 0$). The sign of $\det A$ is directly related to the number of $\mathbf{P}$-modes. In fact, according to the index theorem [13], when two $\mathbf{P}$-modes are present they are both nodes or foci of the dynamics ($\det A > 0$), whereas when four of them are present three are nodes or foci and one is a saddle ($\det A < 0$). More detailed information is obtained by drawing, in the (θ, ϕ) plane, the lines ($\det A = 0$) and ($\mathrm{tr}A = 0, \det A > 0$), which delimit the regions of existence of stable, unstable, and saddle $\mathbf{P}$-modes (Fig. 1).

Stable nodes or foci are the only $\mathbf{P}$-modes that can be physically realized. When no $\mathbf{P}$-mode is stable, there will exist (at least) one attracting limit cycle in the dynamics (Poincaré-Bendixson theorem [14]). A limit cycle represents a periodic $\mathbf{m}$ motion along a closed path on the unit

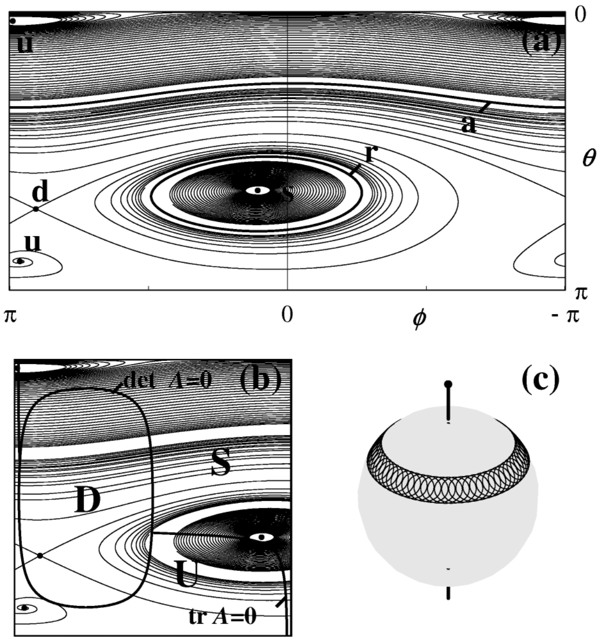

FIG. 1. (a) Example of a LLG phase portrait in the rotating frame for a thin film with ($\alpha = 0.05, \kappa_{\mathrm{eff}} = -1$) at ($h_{az} = 0.6$, $h_{a\perp} = 0.15$, $\omega = 1.1$). The solid points represent stable (s), unstable (u), and saddle (d) **P**-modes. The bold continuous lines are attracting (a) and repelling (r) limit cycles. (b) Lines ($\det A = 0$) and ($\mathrm{tr} A = 0, \det A > 0$) dividing $0 \leq \phi \leq \pi$ hemisphere into regions (S, U, D) of existence of stable, unstable, and saddle **P**-modes, respectively. (c) **Q**-mode associated with limit cycle a, as it appears in the laboratory frame.

sphere. This conclusion holds in the rotating frame. In the laboratory frame, the periodic motion along the limit cycle has to be combined with the rotation of the reference frame and this results in a *quasiperiodic magnetization mode* (**Q**-mode). The quasiperiodicity arises because the external field and the limit cycle periods are not usually commensurable. **Q**-modes spontaneously break the rotational symmetry of the problem by a definite choice for the initial phase of the limit cycle motion.

The following argument proves that **Q**-modes are necessarily present under appropriate conditions. Let us consider the limit $|b_\perp| \to 0$ of small rotating field amplitudes. According to Eqs. (5)–(8), in this limit **P**-modes are characterized by $m_z^2 \to 1$, $\det A \simeq (v^2 + \Omega^2)/(1 + \alpha^2)$, and $\mathrm{tr} A \simeq -2\alpha(\kappa_{\mathrm{eff}} \pm h_{az})/(1 + \alpha^2)$. Only two **P**-modes are possible, because $\det A > 0$. Furthermore, the sign of $\mathrm{tr} A$ is opposite to that of κ_{eff} for both modes in the interval $|h_{az}| < |\kappa_{\mathrm{eff}}|$. Therefore both **P**-modes are unstable for any system with negative κ_{eff} and a **Q**-mode will necessarily set in. This formal result has an intuitive physical interpretation. Let us assume that $\kappa_{\mathrm{eff}} < 0$ and that only the field $h_{az} < |\kappa_{\mathrm{eff}}|$ is applied, i.e., $h_{a\perp} = 0$. In this case, there exists a continuous set of static equilibrium states with $\cos\theta = h_{az}/|\kappa_{\mathrm{eff}}|$ and arbitrary ϕ. In the rotating frame, these states appear as a limit cycle of period $2\pi/\omega$. When a small rotating field $h_{a\perp}$ is applied, the static state is changed into a quasiperiodic motion. In fact, the rotating field is not strong enough to force **m** into synchronous rotation. The magnetization follows the field only for a small part of each rotation period and then periodically falls off synchronism. The result is a slow average **m** precession around the z axis, accompanied by a nutation of frequency ω (see Fig. 1). When $h_{a\perp}$ exceeds only a certain threshold, **m** gets locked to the field and the **Q**-mode is destroyed in favor of a stable **P**-mode.

Figure 1 shows an example of an LLG phase portrait in the rotating frame, calculated by numerical integration of Eqs. (2) and (3). The portrait structure is remarkably rich, with four **P**-modes and two **Q**-modes. In particular, stable **P**-modes and **Q**-modes coexist, a fact that will result in experiments in hysteretic jumps between **P**-type and **Q**-type responses. We have found that a surprisingly broad variety of phase portraits is present in the dynamics. The analysis of this aspect is of considerable complexity and will be presented in detail elsewhere. An example of a bifurcation diagram is shown in Fig. 2. Phase portraits with two or four **P**-modes and zero, one, or two **Q**-modes are present in various combinations, separated by bifurcation lines of saddle-node, Andronov-Hopf, homoclinic-saddle-connection, or semistable-limit-cycle types [15,16]. At a saddle-node bifurcation point, a saddle-node pair of **P**-modes is created or destroyed. This can occur only if $\det A = 0$. By equating Eq. (7) to zero and by plugging the two ensuing $v(m_z)$ roots into Eqs. (5) and (6), one gets the continuous line of Fig. 2. In an Andronov-Hopf bifurcation, a nonsaddle **P**-mode changes from stable to unstable or vice versa, with the simultaneous creation or destruction of a limit cycle. This bifurcation occurs for ($\mathrm{tr} A = 0, \det A > 0$) (dashed lines in Fig. 2). Limit cycles are also created or destroyed in homoclinic-saddle-connection and semistable-limit-cycle bifurcations. However, these bifurcations have a global

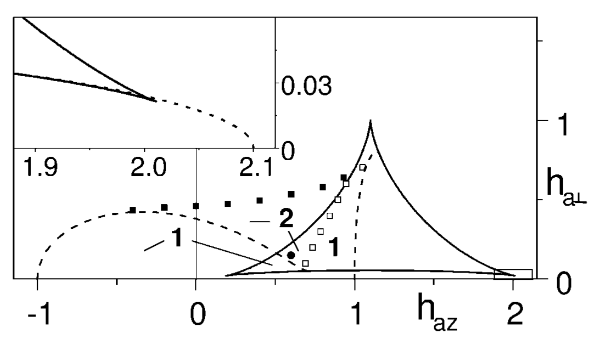

FIG. 2. Bifurcation diagram in ($h_{az}, h_{a\perp}$) control plane for a thin film with ($\alpha = 0.05, \kappa_{\mathrm{eff}} = -1$) at $\omega = 1.1$. Saddle-node (solid line), Andronov-Hopf (dashed line), homoclinic-saddle-connection (open squares), and semistable-limit-cycle (solid squares) bifurcation lines are shown. Values 1 and 2 express the number of **Q**-modes present in different regions. The solid circle shows the location of the phase portrait in Fig. 1. Inset: detail of region relevant to ferromagnetic resonance. The dashed line is the locus of maximum absorbed power.

character, not expressible in terms of local conditions on individual **P**-modes [15,16].

The ($\det A = 0$) line delimits the $(h_{az}, h_{a\perp})$ region, where four **P**-modes exist. This region is the dynamic generalization of the Stoner-Wohlfarth astroid [11] and reduces to it in the limit $\omega \to 0$. In fact, by inserting the two roots of Eq. (7) into Eqs. (5) and (6) and by taking the limit $\omega \to 0$, one obtains the two lines $[b_z = -m_z^3, |b_\perp| = (1 - m_z^2)^{3/2}]$ and $[b_z = -m_z, |b_\perp| = 0]$. The former is just the astroid line $b_z^{2/3} + |b_\perp|^{2/3} = 1$.

The region around the lower right-hand corner of the dynamic astroid of Fig. 2 corresponds to the physical conditions under which ferromagnetic resonance experiments [3] are carried out: $h_{a\perp} \ll 1, h_{az} + \kappa_{\text{eff}} \sim \omega$. Nonlinearities may affect the resonant response even under uniform magnetization, in particular through the appearance of foldover [17] in the absorbed power p. At fixed ω, this results in the fact that the function $p(h_{az})$ ceases to be single valued and the system irreversibly jumps from high to low absorbed power or vice versa when h_{az} is increased or decreased. Foldover is possible when four **P**-modes exist and two of them are stable. The irreversible jumps take place at the ($\det A = 0$) boundary, when one of the two stable modes is destroyed by the saddle-node bifurcation. The $p(h_{az})$ function can be exactly calculated [9]. A **P**-mode is characterized by [see Eq. (4)]

$$h_{az}(m_z) = \omega - \kappa_{\text{eff}} m_z \pm m_z \sqrt{\frac{h_{a\perp}^2}{1 - m_z^2} - \alpha^2 \omega^2}\,, \tag{9}$$

whereas $p(m_z) = \mathbf{h}_{a\perp} \cdot d\mathbf{m}_\perp/dt = \alpha\omega^2(1 - m_z^2)$. The desired $p(h_{az})$ curve can be expressed in the parametric form $[h_{az}(m_z), p(m_z)]$, with m_z as an independent variable decreasing from one down to the value where the square root term of Eq. (9) becomes zero and the absorbed power reaches its maximum. According to Eq. (9), this occurs for $h_{a\perp} = \alpha\omega\sqrt{1 - (h_{az} - \omega)^2/\kappa_{\text{eff}}^2}$ (see Fig. 2). The presence in Eq. (9) of two $h_{az}(m_z)$ branches opens the possibility of foldover. However, foldover is actually realized only if $h_{a\perp}$ exceeds the threshold given by the ordinate of the vertex of the dynamic astroid of Fig. 2. At that vertex, the two $v(m_z)$ roots of the equation $\det A = 0$ coincide. According to Eq. (7), this means that $(1 - m_z^2) = 2|\Omega| m_z$, i.e., $m_z = -|\Omega| + (1 + \Omega^2)^{1/2}$, and $v = (1 - m_z^2)/2$. By inserting these expressions into Eq. (6), one finds for the threshold the exact result [18]

$$h_{a\perp}^2 = \frac{4(\alpha\omega)^3}{|\kappa_{\text{eff}}|} \frac{\sqrt{1 + \Omega^2}}{(\sqrt{1 + \Omega^2} + |\Omega|)^2}\,. \tag{10}$$

The authors wish to thank Pavel Kabos, Carl Patton, and Gary Friedman for helpful discussions. This research was supported in part by the U.S. Department of Energy, Engineering Research Program.

[1] H. B. Callen, J. Phys. Chem. Solids **4**, 256 (1958), and references therein.
[2] W. F. Brown, Jr., *Magnetostatic Principles in Ferromagnetism* (North-Holland, Amsterdam, 1962), Chap. 9.
[3] See *Nonlinear Phenomena and Chaos in Magnetic Materials,* edited by P. E. Wigen (World Scientific, Singapore, 1994), and references therein.
[4] T. J. Silva *et al.,* J. Appl. Phys. **85**, 7849 (1999); G. M. Sandler *et al.,* J. Appl. Phys. **85**, 5080 (1999).
[5] H. Suhl, IEEE Trans. Magn. **34**, 1834 (1998); V. L. Safonov and H. N. Bertram, J. Appl. Phys. **87**, 5508 (2000); D. R. Fredkin and A. Ron, Phys. Rev. B **61**, 8654 (2000).
[6] H. Suhl, J. Phys. Chem. Solids **1**, 209 (1957).
[7] C.-R. Chang and C.-M. Lee, J. Appl. Phys. **83**, 6593 (1998).
[8] H. Suhl and X. Y. Zhang, Phys. Rev. Lett. **57**, 1480 (1986); L. F. Alvarez, O. Pla, and O. Chubykalo, Phys. Rev. B **61**, 11 613 (2000).
[9] G. V. Skrotskii and Iu I. Alimov, Sov. Phys. JETP **35**, 1035 (1959); Sov. Phys. JETP **36**, 899 (1959).
[10] L. R. Walker, Phys. Rev. **105**, 390 (1957); A. Aharoni, J. Appl. Phys. **69**, 7762 (1991).
[11] E. C. Stoner and E. P. Wohlfarth, Philos. Trans. R. Soc. A **240**, 599 (1948); G. Bertotti, *Hysteresis in Magnetism* (Academic, Boston, 1998), Sec. 8.1.
[12] I. D. Mayergoyz, G. Bertotti, and C. Serpico, J. Appl. Phys. **87**, 5511 (2000).
[13] L. Perko, *Differential Equations and Dynamical Systems* (Springer-Verlag, New York, 1996), Sec. 3.12.
[14] S. Wiggins, *Introduction to Applied Nonlinear Dynamical Systems and Chaos* (Springer-Verlag, New York, 1990), Sec. 1.1; J. H. Hubbard and B. H. West, *Differential Equations: A Dynamical System Approach. Part II* (Ref. [15]), Sec. 8*.5.
[15] J. H. Hubbard and B. H. West, *Differential Equations: A Dynamical System Approach. Part II* (Springer-Verlag, New York, 1995).
[16] Y. A. Kuznetsov, *Elements of Applied Bifurcation Theory* (Springer-Verlag, New York, 1995).
[17] D. J. Seagle, S. H. Charap, and J. O. Artman, J. Appl. Phys. **57**, 3706 (1985); Y. K. Fetisov, C. E. Patton, and V. T. Sygonach, IEEE Trans. Magn. **35**, 4511 (1999).
[18] See P. W. Anderson and H. Suhl, Phys. Rev. **100**, 1788 (1955), where the estimate $h_{a\perp}^2 \simeq 3.08(\alpha\omega)^3$ was obtained for a thin-film disk through an approximate linear analysis.